Available online at www.sciencedirect.com

ScienceDirect

www.elsevier.com/locate/jes

JES

JOURNAL OF
ENVIRONMENTAL
SCIENCES

www.jesc.ac.cn

Chlorination of para-substituted phenols: Formation of α, β-unsaturated C$_4$-dialdehydes and C$_4$-dicarboxylic acids

*Zhuoyue Zhang, Carsten Prasse**

Department of Environmental Health and Engineering, Johns Hopkins University, Baltimore, MD 21218, USA

ABSTRACT

Despite the widespread occurrence of phenols in anthropogenic and natural compounds, their fate in reactions with hypochlorous acid (HOCl), one of the most common water treatment disinfectants, remains incompletely understood. To close this knowledge gap, this study investigated the formation of disinfection by-products (DBPs) in the reaction of free chlorine with seven *para*-substituted phenols. Based on the chemical structures of the DBPs and the reaction mechanisms leading to their formation, the DBPs were categorized into four groups: chlorophenols, coupling products, substituent reaction products, and ring cleavage products. In contrast to previous studies that investigated the formation of early-stage chlorophenols, the primary focus of this study was on the elucidation of novel ring cleavage products, in particular α, β-unsaturated C$_4$-dialdehydes, and C$_4$-dicarboxylic acids, which, for the first time, were identified and quantified in this study. The molar yields of 2-butene-1,4-dial (BDA), one of the identified α, β-unsaturated C$_4$-dialdehydes, varied among the different phenolic compounds, reaching a maximum value of 10.4% for bisphenol S. Molar yields of 2-chloromaleic acid (Cl-MA), one of the identified C$_4$-dicarboxylic acids, reached a maximum value of 30.5% for 4-hydroxy-phenylacetic acid under given conditions. 2,4,6-trichlorophenol (TCP) was shown to be an important intermediate of the parent phenols and the C$_4$-ring cleavage products. Based on the temporal trends of α, β-unsaturated C$_4$-dialdehydes and C$_4$-dicarboxylic acids, their formation is likely attributable to two separate ring cleavage pathways. Based on the obtained results, an overall transformation pathway for the reaction of *para*-substituted phenols with free chlorine leading to the formation of novel C$_4$ ring cleavage products was proposed.

© 2022 The Research Center for Eco-Environmental Sciences, Chinese Academy of Sciences. Published by Elsevier B.V.

Introduction

Chlorination, one of the most widely adopted disinfection methods in drinking water and wastewater treatment, plays a critical role in protecting people from waterborne diseases such as cholera, typhoid and dysentery (Calderon, 2000; Cantor, 1994; Cutler and Miller, 2005; McGuire, 2006). However, chlorine can react with both inorganic and organic compounds that are present in the water to generate unintended disinfection by-products (DBPs), many of which are

known or suspected to be toxic (Plewa et al., 2017; Sedlak and von Gunten, 2011; von Gunten, 2018). Although more than 700 DBPs have been identified to date, these typically contribute less than 50% to the total mass balance of halogenated compounds that are formed (Richardson et al., 2018, 2007; Richardson, 2003). Toxicological and epidemiological studies have demonstrated that the toxic effects of chlorinated water can only partially be accounted for by the commonly known halogenated DBPs, suggesting the relevance of other, so far unrecognized DBPs (Chuang et al., 2019; Han et al., 2021; Li and Mitch, 2018).

Among the known DBP precursors, phenols have been shown to be particularly important due to their widespread occurrence in natural organic matter and anthropogenic compounds and their high reactivity with hypochlorous acid (Aeschbacher et al., 2012; Fiss et al., 2007; Huang et al., 2009). Naturally occurring phenols are formed via biosynthesis by plants or decomposition of organic matter (Michalowicz and Duda, 2007). Tyrosine, for example, is a naturally occurring amino acid present in many peptides, proteins, and algae (Chu et al., 2012; Szajdak and Österberg, 1996), and has been detected in treated wastewater in concentrations up to 27.4 μg/L (Mitch et al., 2009). Anthropogenic phenols are widely used as industrial and agricultural chemicals, including personal care products, plastic additives, and pharmaceuticals, as well as herbicides and insecticides (Bulloch et al., 2015; Michalowicz and Duda, 2007). As a result, anthropogenic phenols such as benzophenones and parabens have been detected in drinking water sources in concentrations in the ng/L - low μg/L range (Gryglik and Gmurek, 2018; Liu et al., 2016; Mao et al., 2016; Rodil et al., 2008). *Para*-substituted phenols are particularly common moieties in many anthropogenic chemicals and naturally occurring alkylphenols (Kahl et al., 1997) and are the focus of this study.

Despite the extensive research on the reaction of phenols with chlorine, previous studies have mainly focused on the formation of DBPs in which the phenolic ring remains intact (Acero et al., 2005; Bourgin et al., 2013; Gao et al., 2018; Ge et al., 2006; Yamazaki et al., 2015). This includes the formation of chlorophenols such as 2- and 4-chlorophenol, 2,4- and 2,6-dichlorophenol and TCP via stepwise electrophilic substitution (ES) (Acero et al., 2005; Gallard and von Gunten, 2002; Ge et al., 2006). However, chlorophenols are only the dominant DBPs when phenols are present at similar concentrations as free chlorine (Burttschell et al., 1959). This is in contrast to conditions commonly found in drinking water treatment where chlorine is present in excess, primarily to provide a chlorine residual to prevent microbial regrowth in the distribution system (Rodriguez and Sérodes, 1998). As such, chlorophenols are likely to be transformed further, which emphasizes the need to identify the formed DBPs, in particular ring cleavage products.

Existing knowledge on ring cleavage products is limited to a small number of well-studied DBPs, such as chloroform and chloroacetic acid, which are known to be of health concern (Bond et al., 2012; Richardson et al., 2018). Although chloroform can explain the major fraction of the DBPs for specific phenols such as *meta*-substituted phenols (*e.g.*, resorcinol), it only accounts for a small fraction (~10%) of DBPs formed during chlorination of *para*-substituted phenols (Gallard and von Gunten, 2002). The same is true for chloroacetic acids, dichloroacetic acid (DiCl-AA) and trichloroacetic acid (TriCl-AA), for which yields of 2% and 20%, respectively, have been observed for *para*-substituted phenols (Gallard and von Gunten, 2002; Ge et al., 2014). As such, there is still considerable uncertainty about the identity of ring cleavage products in chlorination of *para*-substituted phenols.

Traditionally, the identification of DBPs primarily has been performed using gas chromatography – mass spectrometry. This, however, limits the detection to volatile and semi-volatile compounds, whereas non-volatile and low-molecular-weight aliphatic compounds are typically not detected. In addition, previous studies have almost exclusively focused on the formation of halogenated DBPs (Jiang et al., 2020; Li and Mitch, 2018). This is in contrast to recent studies demonstrating the formation of non-halogenated compounds such as α, β-unsaturated C_4-dialdehydes during the chlorination of phenol and substituted phenols (Prasse et al., 2020; Prasse, 2021). To address the knowledge gap related to the formation of ring cleavage products from reactions of *para*-substituted phenols with free chlorine, seven model phenols (methylparaben, 4-hydroxyphenylacetic acid, L-tyrosine, N-acetyl-L-tyrosine, 4-hydroxybenzophenone, bisphenol F and bisphenol S)—widely used as food additives, cosmetic ingredients, pharmaceuticals, plastics additives, or commonly detected microbial and human metabolites—were investigated. The aims of this study were to determine the formation and yields of ring cleavage products formed during chlorination of *para*-substituted phenols and to elucidate the transformation pathways leading to their formation.

1.　Materials and methods

1.1.　Chemicals

4-hydroxybenzophenone (4HBP, CAS no.: 1137-42-4), bisphenol S (BPS, CAS no.: 99-76-3), bisphenol F (BPF, CAS no.: 620-92-8), L-tyrosine (L-T, CAS no.: 60-18-4), 2,4,6-trichlorophenol (TCP, CAS no.: 88-06-2), N-α-acetyl-lysine (NAL, CAS no.: 1946-82-3), dichloroacetic acid (DiCl-AA, CAS no.: 79-43-6), trichloroacetic acid (TriCl-AA, CAS no.: 76-03-9) and 2-chlorofumaric acid (Cl-FA, CAS no.: 19071-21-7) were purchased from Sigma-Aldrich in high purity (>98%). Methylparaben (MP, CAS no.: 99-76-3), 4-hydroxyphenylacetic acid (4HPA, CAS no.: 156-38-7), and N-acetyl-L-tyrosine (NAT, CAS no.: 616-91-1) were purchased from Fisher Scientific (>99%). 2,6-dichloro-1,4-benzoquinone (CAS no.: 697-91-6) was purchased from Alfa Aesar (>97%). Appendix A Table S1 summarizes physicochemical properties and typical applications of the *para*-substituted phenols and TCP studied in this work. Working solutions of chlorine were prepared by diluting a commercial solution of sodium hypochlorite (NaOCl, 5% active chlorine, reagent grade; Fisher Scientific). Sodium hypochlorite was standardized by using N,N-diethyl-phenylenediamine (DPD) colorimetric method (Baird et al., 2017). 2,5-dimethoxy-2,5-dihydrofuran (CAS no.: 332-77-4) from Alfa Aesar (99% purity) was used to synthesize the 2-butene-1,4-dial (BDA) stock solution through hydrolysis in ultrapure water at room temperature for at least 48 hr

(Prasse et al., 2018). Solvents used for analysis, buffer salts and sodium thiosulfate were purchased from Fisher Scientific with purity no less than ACS grade. All experimental and analytical solutions, including stock solutions, were prepared in ultrapure water (resistivity > 18 MΩ/cm) produced with a Milli-Q (Merck) or ELGA (Veolia) water purification system.

1.2. Chlorination experiments

Experiments were performed in capped amber vials on a magnetic stirring plate at room temperature. All experiments were conducted with the same initial concentration of 25 µmol/L for all phenolic compounds in ultrapure water buffered at pH 7.5 using 10 mmol/L borate. The pH was monitored and remained constant during the experiments (pH 7.5±0.2). Before initiating the experiment by adding HOCl (10 µL, 0.5 mol/L conc., final conc. 250 µmol/L) to the reaction solution, an aliquot (1 mL) was transferred into an HPLC vial containing sodium thiosulfate as quencher (2 µL, final conc. 2.5 mmol/L). This sample was used to determine the initial concentration of phenols and to validate that the identified DBPs were only attributable to the reaction of HOCl with phenolic compounds. After the addition of HOCl, aliquots were collected in regular intervals over 24 hr and were treated the same as the control sample. For the analysis of α, β-unsaturated C_4-dialdehydes, which cannot be directly detected by liquid chromatography−high-resolution mass spectrometry (LC-HRMS), 5 µL of NAL was added for derivatization (final conc. 250 µmol/L, equivalent to 10 times the initial concentration of the phenolic compound) and samples were incubated for 24 hr at room temperature prior to LC-HRMS analysis (Prasse et al., 2020). Details about the reaction between α, β-unsaturated C_4-dialdehydes and NAL are shown in Appendix A Fig. S1. All other DBPs were directly detected using LC-HRMS. Additional chlorination experiments with TCP, chloroacetic acids, BDA, and Cl-FA, as well as 3,5-dichlorocatechol and 2,6-dichloro-1,4-benzoquinone, were conducted under the same conditions, except that the reaction time was extended to 30 hr.

1.3. Quantification of TCP and ring cleavage products

BDA was quantified using a standard addition method (5−7 levels; max. added concentration at least one order of magnitude above the sample concentration). The stock solution of BDA (1 mol/L) was obtained by the hydrolysis of 2,5-dimethoxy-2,5-dihydrofuran in water as reported previously (Prasse et al., 2020, 2018; Zoumpouli et al., 2021). Concentrations of other BDA analogs, including chloro-BDA (Cl-BDA) and BDA analogs (BDA-Rs) with the para-substituent retained after ring cleavage were estimated using BDA as a reference standard. TCP, DiCl-AA, TriCl-AA, and Cl-FA were quantified using external matrix-matched calibrations (prepared in 10 mmol/L borate buffer (pH 7.5) and 2.5 mmol/L of sodium thiosulfate). The quantification of Cl-MA was achieved by using its isomer Cl-FA as a reference standard (Jans et al., 2021). Limits of detection and quantification are provided in Appendix A Table S3.

1.4. LC−HRMS analysis

An UltiMate 3000 UHPLC system coupled with electrospray ionization (ESI) and a Q Exactive HF Orbitrap MS system (Thermo Scientific) was used for the analysis of all DBPs including those detected via NAL derivatization. For chromatographic separation, a Phenomenex Synergi Hydro-RP column (4 µm, 80 Å, 1 × 150 mm) was used. External mass calibration was performed every 5 days using a calibration standard like the procedures described previously (Prasse et al., 2020). More details on the LC-HRMS analysis can be found in Appendix A Text S1.

2. Results and discussion

2.1. Characterization of DBPs

Analysis of samples using LC-HRMS revealed the formation of 28 DBPs for BPF, 13 DBPs for BPS, 13 DBPs for MP, 14 DBPs for 4HBP, 16 DBPs for 4HPA, 15 DBPs for L-T, and 5 DBPs for NAT. The retention times, precursor ion m/z (with or without chlorine isotope patterns), fragment ion m/z (MS^2), mass accuracy (less than 5 ppm for precursors, less than 10 ppm for fragments), proposed molecular formulas, proposed chemical structures of the DBPs and identification confidence levels (Schymanski et al., 2014) are summarized in Appendix A Tables S4-10. According to the postulated chemical structures and the involved reactions leading to their formation, DBPs were classified into four different groups: (A) chlorophenols, (B) coupling products, (C) substituent reaction products, and (D) ring cleavage products. As an example, time-course profiles of MP and its DBPs with proposed structures are presented in Fig. 1, and the results observed for the other model compounds are provided in Appendix A Figs. S14, S16, S21, S23, S26, and S29. Based on this classification, the number of DBPs from different model phenolic compounds for each group is summarized in Table 1.

The results further highlighted TCP as a common DBP for all investigated para-substituted phenols except NAT. This is discussed further in Section 2.2. The identification of ring cleavage products, which was the focus of this study, highlighted the formation of previously unrecognized DBPs, α, β-unsaturated C_4-dialdehydes and chlorinated C_4-dicarboxylic acids. The formation of DBPs in each category that was observed for each of the investigated phenolic compounds is discussed in following.

2.1.1. Group A: chlorophenols
Chlorination of MP, 4HPA, L-T, and NAT, which all contain a single phenolic ring, led to the formation of mono- and dichloro-DBPs, which can be attributed to electrophilic substitution (ES) of free chlorine on the phenol ring (Gallard and von Gunten, 2002). As previously reported, the electron-donating effect of the hydroxyl group preferentially orients the chlorine ES to the ortho positions, thus leading to the formation of the mono- and dichloro-phenolic compounds (Curtis et al., 2011; Huang et al., 2017; Mao et al., 2016; Trehy et al., 1986). For L-T ($C_9H_{10}O_3N$), which contains a phenolic ring and a primary amine as chlorine reactive moieties, the reaction of chlorine
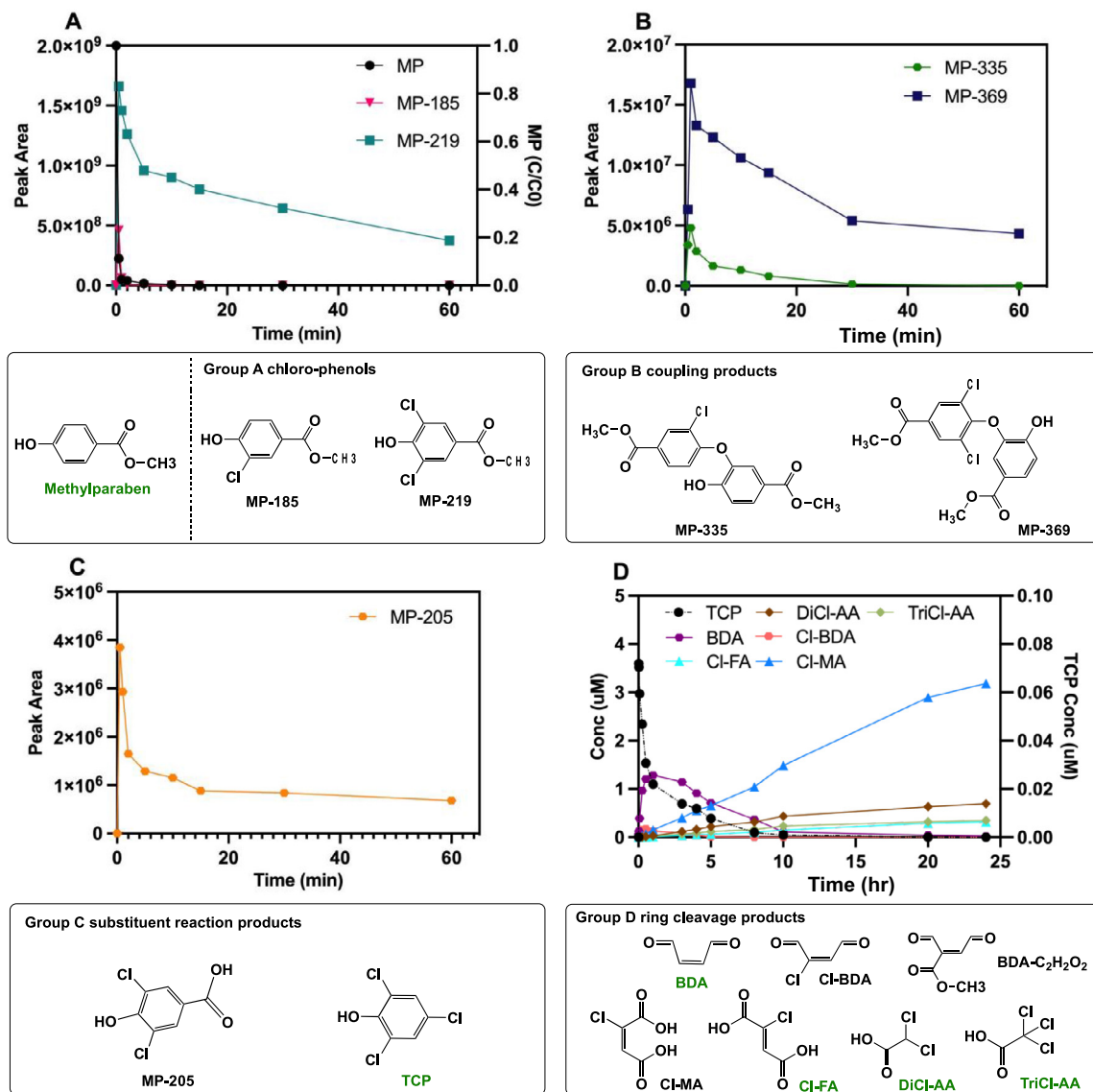
Fig. 1 – Time-course profiles of MP and its chlorination products and proposed chemical structures of chloro-phenols (A), coupling products (B), substituent reaction products (C), and ring cleavage products (D). Compounds labeled in green were confirmed with commercial reference standards. (A), (B) and (C) show results obtained during the reaction of MP with HOCl for 1 hr, while (D) represented quantified concentrations of TCP and the ring cleavage products over 24 hr. Conditions: borate buffer (10 mmol/L); pH 7.5; initial concentration of phenolic compound: 25 μmol/L; initial concentration of HOCl: 250 μmol/L.

Table 1 – Number of DBPs observed for chlorination of investigated para-substituted phenols and their classification into the four DBP categories for each group and the total number of DBPs detected from chlorination of different phenolic compounds. Conditions: borate buffer (10 mmol/L); pH 7.5; initial concentration of phenolic compound: 25 μmol/L; initial concentration of HOCl; 250 μmol/L; sodium thiosulfate concentration: 2.5 mmol/L; NAL concentration: 250 μmol/L.

No. of DBPs		4HBP	BPF	BPS	4HPA	MP	L-T	NAT
Group A	Chlorophenols	4	4	4	2	2	2	2
Group B	Coupling products	0	13	0	2	2	0	0
Group C	Substituent reaction products	3	5	3	6	2	9	0
Group D	Ring cleavage products	7	6	6	6	7	4	3
Total number		14	28	13	16	13	15	5

with the phenolic ring was further supported by MS^2 results of the identified DBPs (Appendix A Table S9). For example, the presence of fragment ion m/z 197.0011 ($C_9H_6O_3Cl$) from L-T214 and fragment ion m/z 230.9619 ($C_9H_5O_3Cl_2$) from L-T248, corresponding to the loss of NH_3, indicates that the primary amine remained unmodified.

For BPS and BPF, which contain two phenolic rings, ES at the *ortho* positions resulted in the formation of mono- to tetrachloro-BPS/BPF as reported previously (Gao et al., 2018; Zheng et al., 2016). For 4HBP, in addition to mono- and dichloro-4HBP (4HBP-231 & 4HBP-265), attributable to chlorine ES on the phenolic ring at the *ortho* positions, DBPs containing three (4HBP-299) and four chlorine atoms (4HBP-333) were observed. This is in agreement with the formation of tri- and tetrachloro-4HBP reported in the literature (Liu et al., 2016) and can be explained by the electron-withdrawing effect of the ketone bridge in 4HBP, which orients the chlorine substitution to *meta* positions on the benzyl ring. Chlorophenols identified for the different *para*-substituted phenols formed rapidly in the first few minutes followed by a subsequent decay indicating further transformation into other DBPs.

2.1.2. Group B: coupling products

Results from LC-HRMS analysis demonstrated the formation of 13 coupling products for BPF, two coupling products for MP, and two coupling products for 4HP. In contrast, no coupling products were observed for BPS, 4HBP, L-T and NAT. The formation of coupling products can most likely be attributed to the formation of phenoxy radicals, which are formed through single-electron transfer (ET) reactions (Xiang et al., 2020; Xu et al., 2010). This is discussed in further detail in Section 2.4.

For BPF ($C_{13}H_{12}O_2$), the coupling products could be further distinguished based on the number of carbons that each DBP contains (i.e., 19 carbons (C_{19}), 26 carbons (C_{26}), and 32 carbons (C_{32})). This includes dichloro- to hexachloro-C_{19} coupling products, BPF-359 ($C_{19}H_{13}O_3Cl_2$), BPF-393 ($C_{19}H_{12}O_3Cl_3$), BPF-427 ($C_{19}H_{11}O_3Cl_4$), BPF-461 ($C_{19}H_{10}O_3Cl_5$) and BPF-495 ($C_{19}H_9O_3Cl_6$) (MS^2 spectra in Appendix A Fig. S13B-F). The MS^2 spectra of these C_{19} coupling products revealed the presence of a common fragment ion, m/z 175.9433 ($C_6H_2O_2Cl_2$), indicating the presence of 2,6-dichlorobenzene-1,4-diol moiety (C_6). The presence of dichloro- to hexachloro-C_{26} coupling products, BPF-465 ($C_{26}H_{19}O_4Cl_2$), BPF-499 ($C_{26}H_{18}O_4Cl_3$), BPF-533 ($C_{26}H_{17}O_4Cl_4$), BPF-567 ($C_{26}H_{16}O_4Cl_5$) and BPF-601 ($C_{26}H_{15}O_4Cl_6$) further indicate the dimerization reaction of two chloro-BPF intermediates (MS^2 spectra in Appendix A Fig. S13G and H). Furthermore, the formation of tetrachloro- to hexachloro-C_{32} coupling products, BPF-625 ($C_{32}H_{21}O_5Cl_4$), BPF-659 ($C_{32}H_{20}O_5Cl_5$), and BPF-693 ($C_{32}H_{19}O_5Cl_6$) (Appendix A Table S4) suggests that the coupling reactions occurred between dimerized chloro-BPFs (C_{26}) and the 2,6-dichlorobenzene-1,4-diol moiety. Similar results have been previously reported by Zheng et al. (2016).

For MP and 4HPA, monochloro to dichloro coupling products were detected (4HPA-335/MP-335; $C_{16}H_{12}O_6Cl$ and 4HPA-369/MP-369; $C_{16}H_{11}O_6Cl_2$). As shown in Appendix A Table S6, the fragment ion m/z 303.0067 ($C_{15}H_8O_5Cl$) observed for MP-335 (Appendix A Fig. S18A) indicates the loss of CH_4O that corresponds to the presence of a methoxy group. Fragment ion m/z 275.0116 ($C_{14}H_8O_4Cl$) further indicates the cleavage of CO

and thus the presence of a carbonyl moiety, while fragment ions m/z 245.0013 ($C_{13}H_6O_3Cl$) and m/z 215.9985 ($C_{12}H_5O_2Cl$) indicate the presence of a second methyl formate group in MP-335. In conclusion, the MS^2 fragment data indicate that MP-335 is a monochloro-MP coupling product. Similar fragment information was observed for MP-369 (Appendix A Fig. S18B), suggesting its structure as a dichloro-MP coupling product. Furthermore, the detection of fragment ion m/z 159.9487 ($C_6H_2OCl_2$) for MP-369 clearly indicates that the dichloro-substitution occurred at the same phenolic ring.

As illustrated in Fig. 1B for monochloro- and dichloro-MP coupling products and the time-course profiles of coupling products for BPF (Appendix A Fig. S14B) and 4HPA (Appendix A Fig. S21B), most of the group B coupling products showed similar temporal trends as the chlorophenols with maximum concentrations within the first 5 min, after which they were transformed further. In contrast, the C_{32}-coupling products from BPF behaved differently and accumulated over the first 15 min and then remained constant.

2.1.3. Group C: substituent reaction products

As shown in Table 1, substituent reaction products were identified for all investigated *para*-substituted phenols except NAT. The formation of substituent reaction products is attributable to oxidation, hydrolysis, and decarboxylation reactions of the substituents (Deborde and von Gunten, 2008; Gao et al., 2018). Among the products, TCP was the only DBP that was detected for all investigated *para*-substituted phenols for which substituent reaction products were observed. The formation of TCP can likely be attributed to the reaction of chlorine with the carbon atom connecting the phenolic ring with the *para* substituent (Gao et al., 2018; Larson and Rockwell, 1979, 2002; Sarkanen and Dence, 1960). The reaction of TCP with free chlorine and its relevance for the formation of ring cleavage products is discussed in further detail in Section 2.2. The identity and formation mechanisms of other substituent reaction products observed for the individual *para*-substituted phenols are discussed in the following.

For BPF, the results indicate that the reaction of chlorine with the methylene bridge connecting the two phenolic rings results in its hydrolytic cleavage, leading to the formation of four substituent reaction products (BPF-191, BPF-189, BPF-155, BPF-205). BPF-191 ($C_7H_5O_2Cl_2$) was tentatively identified as 3,5-dichloro-4-hydroxybenzyl alcohol based on the obtained MS and MS^2 information. In addition, the formation of its aldehyde analog 3,5-dichloro-4-hydroxybenzaldehyde (BPF-189; $C_7H_3O_2Cl_2$) as well as the monochlorinated analog of BPF-189 (BPF-155; $C_7H_4O_2Cl$), 3-chloro-4-hydroxybenzaldehyde was observed (Appendix A Table S4). The formation of these DBPs agrees with previous studies on the chlorination of BPF (Zheng et al., 2016). In addition, the results showed the formation of another, previously unreported DBP, BPF-205 ($C_7H_3O_3Cl_2$). The exact mass information of BPF-205 indicates the presence of an additional oxygen atom compared to BPF-189, and the MS^2 spectrum (Appendix A Fig. S13A) showed the main fragment ion m/z 160.9571 ($C_6H_3OCl_2$), which is formed via cleavage of CO_2, thus suggesting the presence of a carboxylic acid moiety in the molecule. As such, BPF-205 was tentatively identified as 3,5-dichloro-4-hydroxybenzoic acid. These results indicate that

the cleavage of the methylene bridge leads to BPF-191 followed by sequential oxidation of the alcohol moiety of BPF-191 to its aldehyde (BPF-189) and carboxylic acid analog (BPF-205) which is also supported by the temporal trends observed for the formation of these DBPs (Appendix A Fig. S14).

Interestingly, DBPs with the same exact mass and MS^2 results as BPF-191, BPF-189, and BPF-205 were also observed for 4HPA (4HPA-191, 4HPA-189, and 4HPA-205; Appendix A Table S7, Fig. S20B), thus indicating the formation of 3,5-dichloro-4-hydroxybenzyl alcohol, 3,5-dichloro-4-hydroxybenzaldehyde, and 3,5-dichloro-4-hydroxybenzoic acid, respectively. These results demonstrate that chlorination leads to cleavage of the carboxylic acid group, which is in agreement with previous studies showing decarboxylation reactions during chlorination of *para*-hydroxy benzoic acid, styrene, and syringic acid (Larson and Rockwell, 1979; Norwood et al., 1980; Sarkanen and Dence, 1960).

As for MP, the formation of MP-205 indicated the reaction of chlorine with the methoxy group. The MS^2 data of MP-205 (Appendix A Table S6) was very similar to that of BPF-205 and 4HPA-205 and thus was tentatively identified as 3,5-dichloro-4-hydroxybenzoic acid. Its formation can likely be attributed to the hydrolysis of the methoxy group of dichloro-MP (Mao et al., 2016). For BPS, two DBPs, BPS-207 ($C_6H_4O_4ClS$) and BPS-241 ($C_6H_3O_4Cl_2S$) were detected (Appendix A Table S5). For BPS-241, the MS2 information indicates the cleavage of a SO_2 group and thus the presence of a sulfonate moiety (Li and Chen, 2015). For BPS-207, its assigned chemical composition indicated that it is the monochloride analog of BPS-241. Due to its low abundance, however, MS^2 data was not available. The formation of both DBPs can be explained by hydrolysis of the sulfonyl bridge connecting the two phenolic rings in BPS (Gao et al., 2018).

For L-T, three DBPs, L-T166 (C_8H_5ONCl), L-T200 ($C_8H_4ONCl_2$), and L-T203 ($C_8H_5O_2Cl_2$), were identified (Appendix A Table S9). Their formation can be explained by decarboxylation reactions which have also been postulated in previous studies (Chu et al., 2012; Hsu and Shimizu, 1977; Trehy et al., 1986). In addition, three DBPs that have not been reported before were observed (L-T232, L-T215, and L-T249; Appendix A Table S9, Fig. S25). However, information obtained from LC-HRMS was inconclusive and did not provide sufficient information to postulate reasonable chemical structures. For 4HBP, two products 4HBP-121 ($C_7H_5O_2$) and 4HBP-155 ($C_7H_4O_2Cl$) were detected which indicate the cleavage of the ketone bridge during chlorination (Appendix A Table S8). For 4HBP-155, its fragment ion m/z 110.9994 (C_6H_4Cl) indicates the loss of CO_2 and therefore was tentatively identified as chlorobenzoic acid. In contrast to previous studies reporting the formation of a DBP that has one more oxygen atom than dichloro-4HBP (Liu et al., 2016), the formation of the compound was not detected under the investigated experimental conditions.

2.1.4. *Group D: ring cleavage products*

Elucidation of DBPs resulting from the cleavage of the phenolic ring revealed the formation of known ring cleavage products, in particular DiCl-AA and TriCl-AA, as well as several novel products. These newly identified products consist of α, β-unsaturated C_4-dialdehydes and C_4-dicarboxylic acids,

which, to the best of our knowledge, have not been reported before for chlorination of phenols. The formation of DiCl-AA and TriCl-AA, which were confirmed by comparison with commercial reference standards, is in accordance with previous studies investigating the chlorination of phenols (Bond et al., 2012; Ge et al., 2014).

In addition, α, β-unsaturated C_4-dialdehydes BDA and Cl-BDA, which were recently shown to be formed during the reaction of phenol and methyl phenols with free chlorine and hydroxyl radicals (Prasse et al., 2020, 2018), were identified through detection of their corresponding NAL adducts (m/z 253.1193, $C_{12}H_{17}O_4N_2$; m/z 287.0805, $C_{12}H_{16}O_4N_2Cl$) (MS^2 spectra in Appendix A Figs. S2 and S3). BDA and Cl-BDA were detected in chlorination experiments with all investigated *para*-substituted phenols except L-T and NAT (see below for details). BDA and Cl-BDA reached maximum concentrations within the first 1-3 hr and then decayed gradually under the given conditions. The fact that Cl-BDA always reached its maximum earlier than BDA and decayed afterward supports that Cl-BDA is a potential precursor of BDA as proposed by Prasse et al. (2020). Moreover, BDA-Rs, BDA analogs with a *para*-substituent retained, were detected as BDA-C_7H_4O, BDA-$C_2H_2O_2$ and BDA-$C_5H_7NO_3$ for 4HBP, MP and NAT, respectively. The identification of these α, β-unsaturated C_4-dialdehydes are supported by the MS^2 spectra of their corresponding NAL adducts (Appendix A Figs. S4-6).

Furthermore, C_4-dicarboxylic acids were identified as previously unrecognized ring cleavage products for the reaction of chlorine with *para*-substituted phenols. Results from LC-HRMS analysis revealed the formation of two DBPs with the same exact mass (m/z 148.9635; $C_4H_2O_4Cl$) but at different retention times ($\sim$2.2 min and $\sim$4.4 min) in experiments with all investigated phenols. The isotope pattern of both compounds indicated the presence of one chlorine atom and the MS^2 spectra showed the cleavage of CO_2, thus suggesting the presence of at least one carboxylic acid moiety (Appendix A Fig. S10). Based on the results, the DBP detected at a retention time of 2.2 min was identified as 2-chlorofumaric acid (Cl-FA) which was confirmed using a reference standard. As the MS^2 spectrum of the second DBP (retention time 4.4 min) showed the same fragmentation pattern, its formation can be attributed to the formation of Cl-MA, an isomer of Cl-FA. Even though this is the first study demonstrating the formation of Cl-MA and Cl-FA in the reaction of phenols with chlorine, both compounds have been detected previously in chlorination experiments with natural organic matter (Cantor, 1994; Rapson et al., 1980). In addition, Cl-MA and Cl-FA have been previously identified for the degradation of phenols by reactive oxygen species such as OH-radicals (Gupta et al., 2002; Jans et al., 2021; Sorokin et al., 1995). Temporal trends of the concentrations of both compounds showed an increase over the entire duration of the experiments (Fig. 1 and Appendix A Figs. S14, S16, S21, S23, S26 and S29).

2.2. *Yields of TCP and ring cleavage products*

As mentioned before, TCP was the only transformation product for which the phenolic ring remained intact that was detected for all investigated *para*-substituted phenols except NAT with yields up to 14.6% for BPS (Table 2). Differences in

Table 2 – Maximum yields of TCP and ring cleavage products during chlorination of model phenols in 24 hr. Missing valuesindicate that no peaks were observed. Conditions: borate buffer (10 mmol/L); pH 7.5; initial concentration of phenolic compound: 25 µmol/L; initial concentration of HOCl; 250 µmol/L; sodium thiosulfate concentration: 2.5 mmol/L; NAL concentration: 250 µmol/L.

Common DBPs max yield (%)	4HBP	BPF	BPS	4HPA	MP	L-T	NAT
TCP	2.4	7.3	14.6	10.3	5.1	0.2	—
BDA	5.4	2.4	10.4	4.8	2.6	—	—
Cl-BDA	0.3	0.4	1.2	0.8	0.7	—	—
BDA-R	< 0.1	—	—	—	< 0.1	—	< 0.1
Cl-MA	30.5	23.1	27.7	14.7	11.6	11.9	0.8
Cl-FA	1.4	3.2	3.8	1.2	0.9	0.3	< 0.3
DiCl-AA	< 0.4	0.9	0.8	< 0.4	2.5	0.8	< 0.4
TriCl-AA	4.2	9.0	7.9	4.0	1.3	4.2	< 0.3

TCP yields are in agreement with previous studies showing the strong dependence on the chemical composition of the *para*-substituent (de Laat et al., 1982; Gallard and von Gunten, 2002). It is well recognized that the substituent influences the electron density of the aromatic ring by inductive and resonance effects (Gallard and von Gunten, 2002; Hansch et al., 1991).

For 4HBP, BPS and MP, their substituents (carbonyl, sulfonyl and ester groups, respectively) are generally recognized as electron-withdrawing groups (Chataigner et al., 2007; Hansch et al., 1991) that decrease the electron density of the phenolic ring and thus the reactivity of the *para*-position. For BPF, 4HPA, L-T and NAT, the direct adjacent substituent is a methylene group, which does not have strong resonance or inductive effects (Hansch et al., 1991). Therefore, MP and 4HBP, in comparison to 4HPA, were expected to have a lower maximum yield of TCP, which aligns well with our observations (Table 2). Additionally, the low yields of TCP for L-T and its absence in experiments with NAT also suggest that steric hindrance, due to the comparatively larger substituents in these phenols, potentially plays a role in ES occurring at the *para*-position. Chlorination of BPS exhibited the highest yield of TCP, which is not surprising considering the presence of two phenolic rings in this compound. In contrast, much lower TCP yields were observed for BPF which indicates other reaction mechanisms are more important for this compound, in particular the formation of coupling products (see Section 2.4).

Yields of the chloroacetic acids DiCl-AA and TriCl-AA ranged from less than 0.4% for NAT to 2.5% for MP and 9.0% for BPF, respectively. The generally lower yields of DiCl-AA in comparison to TriCl-AA were consistent with results obtained by Ge et al. (2014) for chlorination of several *para*-substituted phenols (including 4-chlorophenol, 4-nitrophenol), with reported yields of DiCl-AA and TriCl-AA of 2.5% and 20%, respectively. As suggested previously (Bond et al., 2012; Ge et al., 2014), the significant variance of yields for both chloroacetic acids can likely be explained by the chemical composition of the substituent and the number of phenolic rings which impact the consumption of HOCl before ring cleavage through ES and other reactions. Although it is intuitive to assume that DiCl-AA and TriCl-AA are closely related to each other, both compounds are likely formed via different reaction mechanisms (Bond et al., 2012; Reckhow et al., 1990). This is also supported by additional chlorination experiments on DiCl-AA and TriCl-AA demonstrating that there was no transformation

from one to the other (data not shown). Yields of the novel C_4-dicarboxylic acid Cl-MA ranged from 11.6% to 30.5% for the tested phenols, except for NAT for which a yield of only 0.8% was observed. The yields of its isomer Cl-FA were generally one magnitude lower than those of Cl-MA, ranging from <0.3% to 3.8% for NAT and BPS, respectively. Although it is a different oxidation system, higher yields of Cl-MA compared to Cl-FA have also been reported for catalytic oxidation of phenols by H_2O_2 (Gupta et al., 2002; Jans et al., 2021; Sorokin et al., 1995).

The yields of α, β-unsaturated C_4-dialdehyde BDA varied and the highest yield was for BPS (10.4%). The highest yield of Cl-BDA was also observed for BPS, even though it was almost an order of magnitude lower (1.2%). This is consistent with results reported previously (Prasse et al., 2020). Even though the mechanism leading to the formation of α, β-unsaturated C_4-dialdehydes is still only incompletely understood, the different BDA and Cl-BDA yields observed for the investigated phenolic compounds are likely a result of the substituent effect (inductive and resonance effects on the phenolic ring, steric effects, and/or reactivity of the substituent) as well as the number of phenolic rings in the molecules. Prasse et al. (2020) have reported a maximum BDA yield of 18% from phenol when HOCl was used in large excess (HOCl/phenol ratios of 30:1 to 50:1) and identified TCP as the precursor of BDA. The importance of TCP as the precursor of BDA likely explains the low yields/absence of BDA in experiments with L-T/NAT, as TCP was also only detected in small yields or was absent. Moreover, BDA analogs with the substituent on the *para*-position retained (BDA-R) were detected in low yields (<0.1%) for 4HBP, MP and NAT. Similar results have been reported for chlorination of *para*-cresol and 4-Br-phenol with the formation of BDA-CH_3 and BDA-Br (Prasse et al., 2020). The detection of BDA-Rs indicates that TCP, though important, is not the only precursor for α, β-unsaturated C_4-dialdehydes. Transformation products such as 2,6-dichloro-4-R-phenol (where R represents a substituent) likely also serve as precursors of α, β-unsaturated C_4-dialdehydes.

2.3. Ring cleavage products of TCP

Due to its importance as an intermediate in the chlorination of *para*-substituted phenols, additional chlorination experiments with TCP were conducted to further investigate the
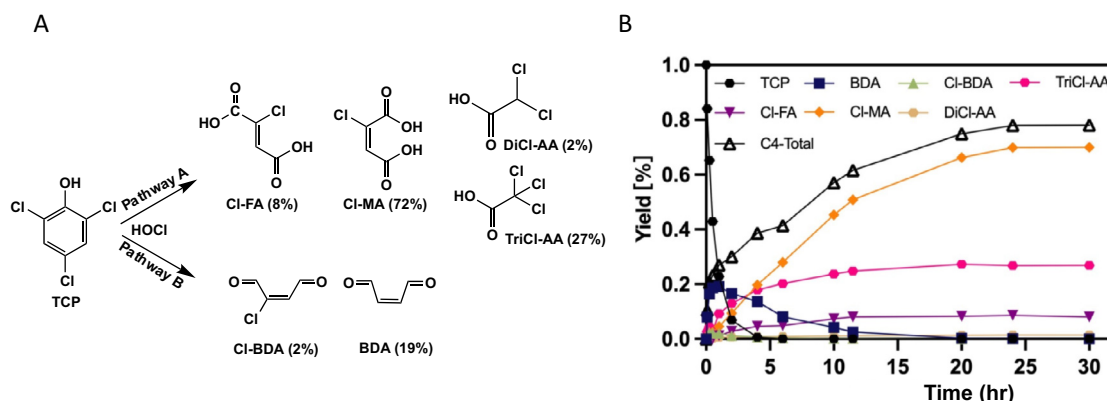
Fig. 2 – (A) Two proposed phenolic ring cleavage pathways of TCP leading to the formation of chlorinated organic acids and α, β-unsaturated C₄-dicarbonyls. The molar yields are quantified or semi-quantified by reference standards. (B) Yield evolution of TCP and its ring cleavage products, together with the total yield of C₄ products (C4_Total), including C₄-α, β-unsaturated dialdehydes and C₄-dicarboxylic acids. Conditions: borate buffer (10 mmol/L); pH 7.5; initial concentration of TCP: 25 µmol/L; initial concentration of HOCl: 250 µmol/L; sodium thiosulfate concentration: 2.5 mmol/L; NAL concentration: 250 µmol/L.

formation of α, β-unsaturated C₄-dialdehydes, C₄-dicarboxylic acids and C₂-carboxylic acids. As expected, reaction with chlorine led to a rapid decrease of TCP while concentrations of DiCl-AA, TriCl-AA, Cl-FA and Cl-MA increased during the first 20 hr and remained constant afterwards. In contrast, BDA and Cl-BDA concentrations increased more rapidly, with maximum concentrations observed after about 1 hr, after which they gradually decreased (Fig. 2B). The temporal trends of Cl-MA, Cl-FA, DiCl-AA and TriCl-AA, which are consistent with their formation trends observed in experiments with the investigated *para*-substituted phenols, indicate that they are formed in parallel. Results further indicate that Cl-MA is the most abundant TCP ring cleavage product with a maximum molar yield of 72% after 24 hr. Maximum molar yields of Cl-FA, BDA, Cl-BDA, DiCl-AA and TriCl-AA were 8% (after 24 hr), 19% (after 1 hr), 2% (after 1 hr), 2% (after 24 hr) and 27% (after 24 hr), respectively. The results for BDA are in agreement with those observed by Prasse et al. (2020) who observed a BDA yield of 18% for TCP. Furthermore, similar yields of DiCl-AA and TriCl-AA have also been reported by Ge et al. (2014).

To investigate whether C₄-dicarboxylic acids can be transformed further to C₂-carboxylic acids, additional chlorination experiments with Cl-FA (HOCl:Cl-FA ratio of 10:1) were performed. The results showed that both DiCl-AA and TriCl-AA are not formed via the degradation of C₄-dicarboxylic acids. Similar results were also observed for chlorination of the α, β-unsaturated dialdehyde BDA, thus demonstrating that the C₄-dicarboxylic acids and C₂-carboxylic acids are formed via different pathways (see Fig. 2A). However, additional studies are needed to further elucidate the reaction mechanisms leading to the formation of the different ring cleavage products. Our results indicate that >80% of the total mass balance of C₄ compounds for TCP can be explained by the newly identified α, β-unsaturated C₄-dialdehydes and C₄-dicarboxylic acids.

In addition to these ring cleavage products that could be quantified, the formation of two additional transformation products, TCP-179 ($C_5H_4O_5Cl$) and TCP-213 ($C_5H_3O_5Cl_2$), was observed. The MS² spectrum of TCP-179 indicated the presence of two carboxylic acid moieties due to the detection of

fragments showing cleavage of 2 x CO₂ (Appendix A Fig. S31). Based on these results, TCP-179 was tentatively identified as 3-chloro-4-hydroxypent-2-enedioic acid. For TCP-213, its assigned chemical composition indicated an extra chlorine substitution for hydrogen on TCP-179. Due to its low abundance, however, MS² data were not available. Even though both DBPs could not be quantified due to the unavailability of reference standards, these results suggest that the formation of C₅-dicarboxylic acids might at least be partially responsible for the remaining mass balance gap of TCP ring cleavage products.

2.4. Overall transformation pathway of para-substituted phenols

Based on the observation of the fate for each phenolic compound and its corresponding DBPs, a general transformation pathway for the reaction of *para*-substituted phenols with free chlorine was proposed (Fig. 3). The transformation pathways for each investigated *para*-substituted phenol are given in Appendix A .

As expected, the obtained results show that the initial reactions with free chlorine involve the formation of mono- and di-chlorophenols via stepwise ES at the *ortho*-positions of the phenols. Subsequent reactions then lead to the substitution of the *para*-substituent and thus the formation of TCP and/or the formation of ring cleavage products. The formation of both can be explained by the reaction of chlorine with phenols via ET, leading to the formation of phenoxy radicals as intermediates (Gao et al., 2018; Larson and Rockwell, 1979). Meanwhile, the phenoxy radicals can react further resulting in the formation of coupling products (Appendix A Fig. S32) (Gao et al., 2018; Xiang et al., 2020). Differences in the formation of coupling products for the tested phenols can be attributed to the characteristics of the *para*-substituents. Although several coupling products were detected for BPF, they were absent in reactions of chlorine with BPS. As demonstrated in previous studies, the stability of radical intermediates is strongly dependent on substituents that
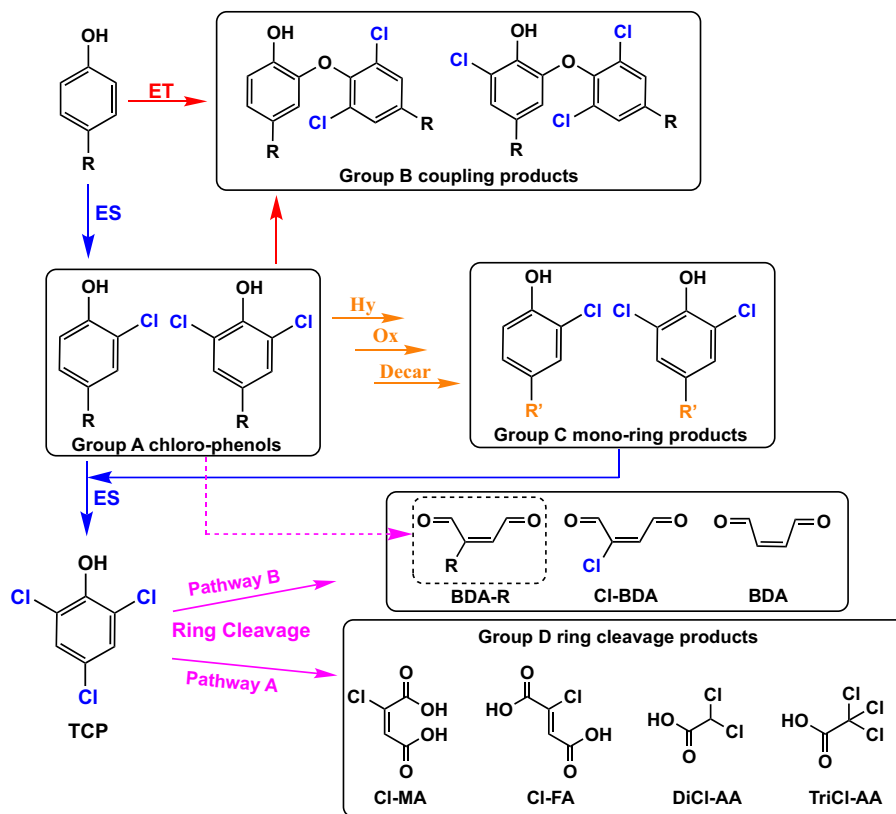
Fig. 3 – Proposed mechanisms for reactions between *para*-substituted phenols and excess free chlorine.

can have either stabilizing or destabilizing effects on the radical intermediates (Bordwell and Cheng, 1991; Creary, 2006; Fisher et al., 1990). The sulfonyl group in BPS is an electron-withdrawing group (Chataigner et al., 2007; Hansch et al., 1991) which results in the stabilization of the radical with the unpaired electron in the *para*-position (see Appendix A Fig. S32 for details). The inability of this radical to react with other radical intermediates explains the absence of coupling products for BPS (Xiang et al., 2020). Instead, as postulated by Gao et al., (2018), the radical intermediate reacts further via cleavage of the substituent. The methylene group in BPF, in contrast, is a weak electron-donating group (Hansch et al., 1991). This stabilizes the BPF radicals with the unpaired electron located at the hydroxyl oxygen or the *ortho*-position which can react with each other to produce BPF dimerized C_{26}-coupling products (Gao et al., 2018; Xiang et al., 2020). The BPF C_{19}-coupling products can be interpreted as coupling reactions between BPF radials (13 carbons) and the radical intermediate formed during cleavage of the sulfonyl group (6 carbons; Appendix A Fig. S32). The latter is also involved in the formation of BPF C_{32}-coupling products via reaction with BPF dimer radicals. The absence of a coupling product for 4HBP, which contains benzaldehyde, known as an electron-withdrawing substituent (Chataigner et al., 2007; Hansch et al., 1991), can be explained by the same mechanism postulated for BPS.

The identification of cleavage products, in particular α, β-unsaturated C_4-dialdehydes and C_4-dicarboxylic acids, and their temporal trends indicate that they are formed through separate reaction pathways. In contrast, DiCl-AA and TriCl-AA

show similar temporal trends as C_4-dicarboxylic acids which indicates that they are formed through the same pathway.

Even though the transformation mechanisms leading to the formation of the ring cleavage products remain incompletely understood, recent work by Prasse et al. (2020, 2018) has suggested the involvement of phenoxy radical intermediates in the formation of α, β-unsaturated C_4-dialdehydes. The involvement of radical intermediates is supported by the detection of the coupling products that are formed via reaction of phenoxy radical intermediates. However, direct evidence for the formation of phenoxy radicals in chlorination systems is still missing. A possible mechanism for phenoxy radical formation involves the intermediate of 3,5-dichlorocatechol, for which the phenoxy radical is generated via direct oxidation by HOCl (Criquet et al., 2015; Guin et al., 2011; Song et al., 2008). 3,5-dichlorocatechol has been shown to react with chlorine to form BDA in high molar yields of 46% (Prasse et al., 2020). Therefore, it is reasonable to propose 3,5-dichlorocatechol as a potential intermediate in the chlorination of TCP responsible for the formation of α, β-unsaturated C_4-dialdehydes. On the other hand, 2,6-dichloro-1,4-benzoquinone, which has been reported previously as a DBP for the reaction of TCP with chlorine (Ge et al., 2008; Kosaka et al., 2017), is unlikely to be a precursor of α, β-unsaturated C_4-dialdehydes. This is supported by the results of chlorination experiments with 2,6-dichloro-1,4-benzoquinone that demonstrated the formation of chlorinated C_4-dicarboxylic acids (Cl-MA, Cl-FA), DiCl-AA and TriCl-AA, while BDA and Cl-BDA were not detected (data not shown). Consequently, 2,6-dichloro-1,4-benzoquinone is

likely to serve as an intermediate between TCP and the chlorinated (di)carboxylic acids. Further studies on the relevance of these potential intermediates during the chlorination of phenols are ongoing.

3.   Conclusions

Our study highlights the importance of ring cleavage products that are formed when chlorine is present in excess, a condition typical for drinking water treatment. This is in contrast to most previous studies that focused primarily on the formation of chlorophenols that are formed initially in the reaction of *para*-substituted phenols with free chlorine. These results revealed the formation of two groups of novel ring cleavage products, chlorinated C_4-dicarboxylic acids and α, β-unsaturated C_4-dialdehydes. Although the toxicity of chlorinated C_4-dicarboxylic acids has not been investigated in detail, the formation of α, β-unsaturated C_4-dialdehydes BDA and Cl-BDA is of considerable concern due to their high toxicity. Our results further demonstrate the role of TCP as an important intermediate in the formation of chlorinated C_4-dicarboxylic acids and α, β-unsaturated C_4-dialdehydes. This highlights the need to investigate the potential health impacts associated with the identified ring cleavage products, especially chlorinated C_4-dicarboxylic acids. Furthermore, additional research is needed to elucidate the reaction mechanisms leading to the formation of chlorinated C_4-dicarboxylic acids and α, β-unsaturated C_4-dialdehydes.

Acknowledgments

Appendix A Supplementary data

Supplementary material associated with this article can be found, in the online version, at doi:10.1016/j.jes.2022.04.029.

REFERENCES

Acero, J.L., Piriou, P., von Gunten, U., 2005. Kinetics and mechanisms of formation of bromophenols during drinking water chlorination: Assessment of taste and odor development. Water Res. 39, 2979–2993.

Aeschbacher, M., Graf, C., Schwarzenbach, R.P., Sander, M., 2012. Antioxidant properties of humic substances. Environ. Sci. Technol. 46, 4916–4925.

Bond, T., Goslan, E.H., Parsons, S.A., Jefferson, B., 2012. A critical review of trihalomethane and haloacetic acid formation from natural organic matter surrogates. Environ. Technol. Rev. 1, 93–113.

Bordwell, F.G., Cheng, J., 1991. Substituent effects on the stabilities of phenoxyl radicals and the acidities of phenoxyl radical cations. J. Am. Chem. Soc. 113, 1736–1743.

Bourgin, M., Bichon, E., Antignac, J.P., Monteau, F., Leroy, G., Barritaud, L., et al., 2013. Chlorination of bisphenol A: non-targeted screening for the identification of transformation products and assessment of estrogenicity in generated water. Chemosphere 93, 2814–2822.

Bulloch, D.N., Nelson, E.D., Carr, S.A., Wissman, C.R., Armstrong, J.L., Schlenk, D., et al., 2015. Occurrence of halogenated transformation products of selected pharmaceuticals and personal care products in secondary and tertiary treated wastewaters from southern California. Environ. Sci. Technol. 49, 2044–2051.

Burttschell, R.H., Rosen, A.A., Middleton, F.M., Ettinger, M.B., 1959. Chlorine Derivatives of Phenol Causing Taste and Odor. J. Am. Water Work. Assoc. 51, 205–214.

Calderon, R.L., 2000. The epidemiology of chemical contaminants of drinking water. Food Chem. Toxicol. 38, S13–S20.

Cantor, K.P., 1994. Water chlorination, mutagenicity, and cancer epidemiology. Am. J. Public Health 84, 1211–1213.

Chataigner, I., Panel, C., Gérard, H., Piettre, S.R., 2007. Sulfonyl vs. carbonyl group: which is the more electron-withdrawing? Chem. Commun. 3288.

Chu, W., Gao, N., Krasner, S.W., Templeton, M.R., Yin, D., 2012. Formation of halogenated C-, N-DBPs from chlor(am)ination and UV irradiation of tyrosine in drinking water. Environ. Pollut. 161, 8–14.

Chuang, Y.-H., Szczuka, A., Mitch, W.A., 2019. Comparison of Toxicity-Weighted Disinfection Byproduct Concentrations in Potable Reuse Waters and Conventional Drinking Waters as a New Approach to Assessing the Quality of Advanced Treatment Train Waters. Environ. Sci. Technol. 53, 3729–3738.

Creary, X., 2006. Super Radical Stabilizers. Acc. Chem. Res. 39, 761–771.

Criquet, J., Rodriguez, E.M., Allard, S., Wellauer, S., Salhi, E., Joll, C.A., et al., 2015. Reaction of bromine and chlorine with phenolic compounds and natural organic matter extracts – Electrophilic aromatic substitution and oxidation. Water Res. 85, 476–486.

Curtis, M.P., Hicks, A.J., Neidigh, J.W., 2011. Kinetics of 3-Chlorotyrosine Formation and Loss due to Hypochlorous Acid and Chloramines. Chem. Res. Toxicol. 24, 418–428.

Cutler, D., Miller, G., 2005. The role of public health improvements in health advances: The twentieth-century United States. Demography 42, 1–22.

de Laat, J., Merlet, N., Dore, M., 1982. Chloration de composés organiques: demande en chlore et réactivite vis-a-vis de la formation des trihalométhanes. Incidence de l'azote ammoniacal. Water Res. 16, 1437–1450.

Deborde, M., von Gunten, U. (Eds.), 2008. Reactions of chlorine with inorganic and organic compounds during water treatment - Kinetics and mechanisms: A critical review, Eds.. Water Res.

Fisher, T.H., Dershem, S.M., Prewitt, M.L., 1990. Meta-substituent effects on benzyl free-radical stability. J. Org. Chem. 55, 1040–1043.

Fiss, E.M., Rule, K.L., Vikesland, P.J., 2007. Formation of Chloroform and Other Chlorinated Byproducts by Chlorination of Triclosan-Containing Antibacterial Products. Environ. Sci. Technol. 41, 2387–2394.

Gallard, H., von Gunten, U., 2002. Chlorination of Phenols: Kinetics and Formation of Chloroform. Environ. Sci. Technol. 36, 884–890.

Gao, Y., Jiang, J., Zhou, Y., Pang, S.Y., Ma, J., Jiang, C., et al., 2018. Chlorination of bisphenol S: Kinetics, products, and effect of humic acid. Water Res. 131, 208–217.

Ge, F., Tang, F., Xu, Y., Xiao, Y., 2014. Formation characteristics of

haloacetic acids from phenols in drinking water chlorination. Water Supply 14, 142–149.

Ge, F., Zhu, L., Chen, H., 2006. Effects of pH on the chlorination process of phenols in drinking water. J. Hazard. Mater. 133, 99–105.

Ge, F., Zhu, L., Wang, J., 2008. Distribution of chlorination products of phenols under various pHs in water disinfection. Desalination 225, 156–166.

Gryglik, D., Gmurek, M., 2018. The photosensitized oxidation of mixture of parabens in aqueous solution. Environ. Sci. Pollut. Res. 25, 3009–3019.

Guin, P.S., Das, S., Mandal, P.C., 2011. Electrochemical Reduction of Quinones in Different Media: A Review. Int. J. Electrochem. 816202.

Gupta, S.S., Stadler, M., Noser, C.A., Ghosh, A., Steinhoff, B., Lenoir, D., et al., 2002. Rapid Total Destruction of Chlorophenols by Activated Hydrogen Peroxide. Science 296, 326–328.

Han, J., Zhang, X., Jiang, J., Li, W., 2021. How much of the total organic halogen and developmental toxicity of chlorinated drinking water might be attributed to aromatic halogenated DBPs? Environ. Sci. Technol. 55 (9), 5906–5916.

Hansch, Corwin., Leo, A., Taft, R.W., 1991. A survey of Hammett substituent constants and resonance and field parameters. Chem. Rev. 91, 165–195.

Huang, G., Jiang, P., Li, X.-F., 2017. Mass Spectrometry Identification of N-Chlorinated Dipeptides in Drinking Water. Anal. Chem. 89, 4204–4209.

Hsu, R.Y., Shimizu, Y., 1977. Phenylpropanoids in Chlorination. Chesapeake Science 18, 129.

Huang, W.Y., Cai, Y.Z., Zhang, Y., 2009. Natural Phenolic Compounds From Medicinal Herbs and Dietary Plants: Potential Use for Cancer Prevention. Nutr. Cancer 62, 1–20.

Jans, U., Prasse, C., von Gunten, U., 2021. Enhanced Treatment of Municipal Wastewater Effluents by Fe-TAML/H$_2$O$_2$: Efficiency of Micropollutant Abatement. Environ. Sci. Technol. 55, 3313–3321.

Jiang, J., Han, J., Zhang, X., 2020. Nonhalogenated aromatic DBPs in drinking water chlorination: a gap between NOM and halogenated aromatic DBPs. Environ. Sci. Technol. 54 (3), 1646–1656.

Kahl, M.D., Makynen, E.A., Kosian, P.A., Ankley, G.T., 1997. Toxicity of 4-Nonylphenol in a Life-Cycle Test with the MidgeChironomus tentans. Ecotoxicol. Environ. Saf. 38, 155–160.

Kosaka, K., Nakai, Hishida, Y., Asami, M., Ohkubo, K., Akiba, M., 2017. Formation of 2,6-dichloro-1,4-benzoquinone from aromatic compounds after chlorination. Water Res. 110, 48–55.

Larson, R.A., Rockwell, A.L., 1979. Chloroform and chlorophenol production by decarboxylation of natural acids during aqueous chlorination. Environ. Sci. Technol. 13, 325–329.

Larson, R.A., Rockwell, A.L., 2002. Chloroform and Chlorophenol Production By Decarboxylation Of Natural Acids During Aqueous Chlorination [WWW Document]. ACS Publ.

Li, M., Chen, Y., 2015. Analysis of Sulfonated Anthraquinone Dyes by Electrospray Ionization Quadrupole Time-of-flight Tandem Mass Spectrometry. J .Textile Sci. Eng. 06.

Li, X.-F., Mitch, W.A., 2018. Drinking water disinfection byproducts (DBPS) and human health effects: multidisciplinary challenges and opportunities. Environ. Sci. Technol. 52, 1681–1689.

Liu, W., Wei, D., Liu, Q., Du, Y., 2016. Transformation pathways and acute toxicity variation of 4-hydroxyl benzophenone in chlorination disinfection process. Chemosphere 154, 491–498.

Mao, Q., Ji, F., Wang, W., Wang, Q., Hu, Z., Yuan, S., 2016. Chlorination of parabens: reaction kinetics and transformation product identification. Environ. Sci. Pollut. Res. Int. 23, 23081–23091.

McGuire, M.J., 2006. Eight revolutions in the history of US drinking water disinfection. J. AWWA 98, 123–149.

Michalowicz, J., Duda, W., 2007. Phenols - sources and toxicity. Pol. J. Environ. Stud. 16, 347–362.

Mitch, W.A., Krasner, S.W., Westerhoff, P., Dotson, A., 2009. Occurrence and Formation of Nitrogenous Disinfection By-Products. American Water Works Association Research Foundation, Denver, Colo.

Norwood, D.L., Johnson, J.D., Christman, R.F., Hass, J.R., Bobenrieth, M.J., 1980. Reactions of chlorine with selected aromatic models of aquatic humic material. Environ. Sci. Technol. 14, 187–190.

Plewa, M.J., Wagner, E.D., Richardson, S.D., 2017. TIC-Tox: A preliminary discussion on identifying the forcing agents of DBP-mediated toxicity of disinfected water. J. Environ. Sci. 58, 208–216.

Prasse, C., 2021. Reactivity-directed analysis – a novel approach for the identification of toxic organic electrophiles in drinking water. Environ. Sci. Process. Impacts 23, 48–65.

Prasse, C., Ford, B., Nomura, D.K., Sedlak, D.L., 2018. Unexpected transformation of dissolved phenols to toxic dicarbonyls by hydroxyl radicals and UV light. Proc. Natl. Acad. Sci. 115, 2311–2316.

Prasse, C., von Gunten, U., Sedlak, D.L., 2020. Chlorination of Phenols Revisited: Unexpected Formation of α,β-Unsaturated C4-Dicarbonyl Ring Cleavage Products. Environ. Sci. Technol. 54, 826–834.

Rapson, W.H., Nazar, M.A., Butsky, V.V., 1980. Mutagenicity produced by aqueous chlorination of organic compounds. Bull. Environ. Contam. Toxicol. 24, 590–596.

Reckhow, D.A., Singer, P.C., Malcolm, R.L., 1990. Chlorination of humic materials: byproduct formation and chemical interpretations. Environ. Sci. Technol. 24, 1655–1664.

Baird, R.B., Eaton, A.D., Rice, E.W., 2017. Standard Methods for the Examination of Water and Wastewater, 23rd Ed. American Public Health Association, American Water Works Association, Water Environment Federation, Washington D.C.

Richardson, S., Ternes, T., Van, D., 2018. Water Analysis: Emerging Contaminants and Current Issues. Anal. Chem. 90.

Richardson, S.D., 2003. Disinfection by-products and other emerging contaminants in drinking water. TrAC Trends Anal. Chem. 22, 666–684.

Richardson, S.D., Plewa, M.J., Wagner, E.D., Schoeny, R., DeMarini, D.M., 2007. Occurrence, genotoxicity, and carcinogenicity of regulated and emerging disinfection by-products in drinking water: A review and roadmap for research. Mutat. Res. Mutat. Res. 636, 178–242 The Sources and Potential Hazards of Mutagens in Complex Environmental Matrices - Part II.

Rodil, R., Quintana, J.B., López-Mahía, P., Muniategui-Lorenzo, S., Prada-Rodríguez, D., 2008. Multiclass Determination of Sunscreen Chemicals in Water Samples by Liquid Chromatography−Tandem Mass Spectrometry. Anal. Chem. 80, 1307–1315.

Rodriguez, M.J., Sérodes, J.-B., 1998. Assessing empirical linear and non-linear modelling of residual chlorine in urban drinking water systems. Environ. Model. Softw. 14, 93–102.

Sarkanen, K.V., Dence, C.W., 1960. Reactions of p-Hydroxybenzyl Alcohol Derivatives and Their Methyl Ethers with Molecular Chlorine. J. Org. Chem. 25, 715–720.

Schymanski, E.L., Jeon, J., Gulde, R., Fenner, K., Ruff, M., Singer, H.P., Hollender, J., 2014. Identifying Small Molecules via High Resolution Mass Spectrometry: Communicating Confidence. Environ. Sci. Technol. 48, 2097–2098.

Sedlak, D.L., von Gunten, U., 2011. The Chlorine Dilemma. Science 331, 42–43.

Song, Y., Buettner, G.R., Parkin, S., Wagner, B.A., Robertson, L.W., Lehmler, H.J., 2008. Chlorination Increases the Persistence of

Semiquinone Free Radicals Derived from Polychlorinated Biphenyl Hydroquinones and Quinones. J. Org. Chem. 73, 8296–8304.

Sorokin, A., Meunier, B., Séris, J.-L., 1995. Efficient Oxidative Dechlorination and Aromatic Ring Cleavage of Chlorinated Phenols Catalyzed by Iron Sulfophthalocyanine. Science 268, 1163–1166.

Szajdak, L., Österberg, R., 1996. Amino acids present in humic acids from soils under different cultivations. Environ. Int. 3, 331–334.

Trehy, M.L., Yost, R.A., Miles, C.J., 1986. Chlorination byproducts of amino acids in natural waters. Environ. Sci. Technol. 20, 1117–1122.

von Gunten, U., 2018. Oxidation Processes in Water Treatment: Are We on Track? Environ. Sci. Technol. 52, 5062–5075.

Xiang, W., Qu, R., Wang, X., Wang, Z., Bin-Jumah, M., Allam, A.A., et al., 2020. Removal of 4-chlorophenol, bisphenol A and nonylphenol mixtures by aqueous chlorination and formation of coupling products. Chem. Eng. J. 402, 126140.

Xu, F., Yu, W., Gao, R., Zhou, Q., Zhang, Q., Wang, W., 2010. Dioxin Formations from the Radical/Radical Cross-Condensation of Phenoxy Radicals with 2-Chlorophenoxy Radicals and 2,4,6-Trichlorophenoxy Radicals. Environ. Sci. Technol. 44, 6745–6751.

Yamazaki, E., Yamashita, N., Taniyasu, S., Lam, J., Lam, P.K.S., Moon, H.-B., et al., 2015. Bisphenol A and other bisphenol analogs including BPS and BPF in surface water samples from Japan, China, Korea and India. Ecotoxicol. Environ. Saf. 122, 565–572.

Zheng, S., Shi, J., Hu, J., Hu, W., Zhang, J., Shao, B., 2016. Chlorination of bisphenol F and the estrogenic and peroxisome proliferator-activated receptor gamma effects of its disinfection byproducts. Water Res. 107, 1–10.

Zoumpouli, G.A., Zhang, Z., Wenk, J., Prasse, C., 2021. Aqueous ozonation of furans: Kinetics and transformation mechanisms leading to the formation of α,β-unsaturated dicarbonyl compounds. Water Res. 203, 117487.